Molecular Therapy
Nucleic Acids
Original Article

Leverage of nuclease-deficient CasX for preventing pathological angiogenesis

Haote Han,[1,7] Yanhui Yang,[2,7] Yunjuan Jiao,[3,4,7] Hui Qi,[5] Zhuo Han,[1] Luping Wang,[1] Lijun Dong,[5] Jingkui Tian,[1] Bart Vanhaesebroeck,[6] Xiaopeng Li,[4] Junwen Liu,[3] Gaoen Ma,[4] and Hetian Lei[4,5]

[1]Institute of Basic Medicine and Cancer, Chinese Academy of Sciences, Cancer Hospital of the University of Chinese Academy of Sciences, Zhejiang Cancer Hospital, Hangzhou 310000, People's Republic of China; [2]Ningxia Key Laboratory of Prevention and Control of Common Infectious Diseases, the School of Basic Medical Sciences, Ningxia Medical University, Yinchuan 750004, People's Republic of China; [3]Department of Histology and Embryology, Xiangya School of Medicine, Central South University, Changsha 410013, People's Republic of China; [4]The Third Affiliated Hospital of Xinxiang Medical University, Xinxiang 453003, China; [5]Shenzhen Eye Hospital, Jinan University, Shenzhen Eye Institute, Shenzhen 518000, People's Republic of China; [6]Cancer Institute, University College London, London NW1 2BU, UK

Gene editing with a CRISPR/Cas system is a novel potential strategy for treating human diseases. Pharmacological inhibition of phosphoinositide 3-kinase (PI3K) δ suppresses retinal angiogenesis in a mouse model of oxygen-induced retinopathy. Here we show that an innovative system of adeno-associated virus (AAV)-mediated CRISPR/nuclease-deficient (d)CasX fused with the Krueppel-associated box (KRAB) domain is leveraged to block (81.2% ± 6.5%) *in vitro* expression of p110δ, the catalytic subunit of PI3Kδ, encoded by *Pik3cd*. This CRISPR/dCasX-KRAB (4, 269 bp) system is small enough to be fit into a single AAV vector. We then document that recombinant AAV serotype (rAAV)1 efficiently transduces vascular endothelial cells from pathologic retinal vessels, which show high expression of p110δ; furthermore, we demonstrate that blockade of retinal p110δ expression by intravitreally injected rAAV1-CRISPR/dCasX-KRAB targeting the *Pik3cd* promoter prevents (32.1% ± 5.3%) retinal p110δ expression as well as pathological retinal angiogenesis in a mouse model of oxygen-induced retinopathy. These data establish a strong foundation for treating pathological angiogenesis by AAV-mediated CRISPR interference with p110δ expression.

INTRODUCTION

The advent of CRISPR/Cas technology has profoundly changed the research field of gene editing and even the entire life sciences.[1] This CRISPR technology originated from a natural bacterial defense mechanism against phage infection and plasmid transfer[2] and is capable of manipulating nearly any genomic sequence specified by a small RNA-guided Cas to work,[2] including correction of disease-causing mutations.[3–6] CRISPR/Cas-mediated genome engineering is expected to become an important tool for the treatment or cure of a variety of human diseases, including but not limited to tumors, neurodegenerative diseases, sickle cell anemia, hereditary diseases, viral infection, immune system disease, and vascular disease.[7–14]

Adeno-associated virus (AAV) has been widely used in gene therapy and vaccine research;[15,16] its packaging capacity is limited to less than 4.7 kb; however, while many CRISPR/Cas systems exceed this limit. CasX, discovered in 2019 by Dr. J. Doudna's research team from the world's smallest bacteria,[17] is a DNA endonuclease consisting of 980 amino acids (aa) that is much smaller than canonical *Streptococcus pyogenes* Cas9 (SpCas9: 1368 aa) and also smaller than *Staphylococcus aureus* Cas9 (1,053 aa).[18,19] CasX specifically cleaves double-stranded DNA with a protospacer adjacent motif (PAM) "TTCN" at the 5′ side under the guidance of single guide RNA (sgRNA). When mutated at Asp672, Glu 769, and Asp935, CasX loses its nuclease activity of cutting DNA, but it retains the ability to bind to target DNA.[17] Such nuclease-deficient CasX is named as dCasX, whose function is similar to dCas9,[20] and is the basis for a CRISPR interference (CRISPRi) system, which can specifically bind to the genomic DNA without disrupting the genomic sequence.

Neovascularization can be the origin of myriad diseases,[21–23] and it is a spiral capillary newly protruding from a normal blood vessel. Such abnormal new blood vessels may lead to specific diseases, collectively referred to as "angiogenesis diseases." These include solid tumors, neovascular age-related macular degeneration, retinopathy of premature, and proliferative diabetic retinopathy (PDR).[24–27] During PDR pathogenesis, retinal hypoxia induces an increase in a variety of genes, including vascular endothelial growth factor (VEGF), erythropoietin, and cytokines, leading to angiogenesis.[28–30] Recent studies showed that inactivation of the phosphoinositide 3-kinase (PI3K) δ isoform inhibits retinal angiogenesis in a mouse model of oxygen-induced retinopathy (OIR).[31] PI3Kδ consists of a catalytic p110δ subunit, encoded by the *Pik3cd* gene, which occurs in complex with a p85

Received 12 December 2022; accepted 3 August 2023;
https://doi.org/10.1016/j.omtn.2023.08.001.

[7]These authors contributed equally

Correspondence: Gaoen Ma, 599 Hualan Road, Xinxiang, Henan province 453003, China.
E-mail: 15757826611@163.com
Correspondence: Hetian Lei, 599 Hualan Road, Xinxiang, Henan province 453003, China.
E-mail: leihetian18@hotmail.com

regulatory subunit.[31] In this study, we aimed to establish a novel AAV vector with CRISPR/dCasX fused with a gene-suppression Krueppel-associated box (KRAB) domain, which is one of transcriptional repression domains appearing in approximately 400 human zinc finger protein-based transcription factors (KRAB zinc finger proteins), and to investigate whether AAV-mediated CRISPR/dCasX-KRAB (hereafter short as CRISPR/dCasX) could be harnessed to block p110δ expression so as to prevent retinal angiogenesis.

RESULTS

CRISPR/dCasX-mediated blockade of p110δ expression *in vitro*

As a low immunogenicity viral vector, AAV is superior to other viral vectors in terms of safety.[15] Compared with CRISPR/Cas-mediated gene knockout technology, CRISPRi has the advantages of not changing the genome sequence of the target gene locus and low off-target effects.[32] Thereby, we created an AAV vector expressing dCasX-KRAB (dCasX) and sgRNA (pAAV-U6-sgRNA/Rous sarcoma virus [RSV]-dCasX (referred to as V3) (Figure 1A).

To examine whether pAAV-RSV-dCasX was correctly constructed, we transfected this vector into human embryonic kidney (HEK) 293T cells. The results showed that dCasX expression was confirmed at 48 h after transfection by immunofluorescence (Figure 1B) and Western blot analyses (Figures 1C and 1D), demonstrating that the promoter of RSV can drive dCasX expression within this construct in mammalian cells.[33,34]

We next examined whether recombinant AAV serotype (rAAV)1 was able to deliver GFP driven by cytomegalovirus (CMV) into human retinal microvascular endothelial cells (HRECs), retinal pigment epithelial cells (ARPE-19), and mouse macrophage cells (RAW264.7), which highly express PI3Kδ[35] and can produce VEGF, a key driver for angiogenesis.[36–39] The results showed that GFP expression in these cells could be detected at 24 h after infection (Figure 2A), suggesting that rAAV1 can be leveraged to deliver the CRISPR/dCasX to these cell types.

To block p110δ expression using the CRISPRi strategy of AAV-CRISPR/dCasX, an sgRNA named as mPK5 for guiding dCasX to bind to the second promoter of murine *Pik3cd* was cloned into this vector (Figure 2B). To evaluate the efficiency of this dCasX system, murine macrophage cells (RAW264.7) were infected with rAAV1 virus carrying the dCasX/sgRNA-mPK5 or a control virus. The results showed that p110δ was reduced by approximately 80% in RAW264.7 infected with rAAV1- dCasX/sgRNA-mPK5 compared with those infected with rAAV1- dCasX/sgRNA-*lacZ* (Figures 2C, 2D, and S1); in addition, experiments of chromatin immunoprecipitation (ChIP) using an antibody against CasX showed that the dCasX could bind to the *Pik3cd* promoter in the RAW264.7 cells infected with rAAV1-dCasX/sgRNA-mPK5 (Figures 2E and S2). In addition, RNA sequencing analysis indicated that dCasX alone affected some gene expression and pathways (Figures S3 and S4), but we failed to find predicted off-target effects from dCasX/sgRNA-mPK5 (Figure S2). These data together document that dCasX under the guidance of sgRNA-mPK5 is capable of specifically binding to the second promoter of *Pik3cd* for hindering p110δ expression.

dCasX delivered by rAAV1 is highly expressed in retinal pigment epithelial cells and pathological retinal vascular ECs *in vivo*

We next explored whether rAAV1-CRISPR/dCasX could efficiently infect p110δ-expressing retinal cells *in vivo*. Thereby, rAAV1-dCasX/sgRNA-*lacZ* was intravitreally into postnatal (P)12 mice, and the mouse eyeballs were collected on days 1, 3, and 5 after injection for immunofluorescence analysis using an antibody against CasX. To determine which tissues expressed CasX, the retinal sections were co-stained with the anti-CasX antibody together with an epithelial cell marker Pankeratin or an endothelial marker isolectin B4. The results showed that dCasX expression was detected on day 1 after injection, its expression was increased on days 3 and 5 (Figure 3A), and that dCasX was mainly expressed in the retinal pigment epithelium layer (Figures 3B and 3E–3H) and weakly expressed in vascular ECs (Figure 3C and 3I–3L) and microglia cells (Figures 3D and 3M–3P).

We next intravitreally injected rAAV1-dCasX/sgRNA-*lacZ* into P12 mice in the mouse model of OIR, and the eyeballs were harvested on P17 in this mouse model. The co-staining results showed that dCasX was strongly expressed in pathological vascular ECs in tufts (pathological vessels) in this OIR mouse model (Figures 4A–4E), suggesting that pathological vascular ECs are more susceptible to rAAV1 infection than normal vascular ECs.

CRISPR/dCasX-mediated blockade of p110δ expression prevents angiogenesis in a mouse model of OIR

We next evaluated whether rAAV1-dCasX/sgRNA-mPK5 could block p110δ expression and prevent neovascularization *in vivo*. To this end, we intravitreally injected equal amounts of rAAV1-dCasX/sgRNA-mPK5 or rAAV1-dCasX/sgRNA-*lacZ* into P12 mice in the OIR model. In this model, P7 pups with nursing mothers are placed in a hyperoxia (75% oxygen) chamber for 5 days, during which central retinal vessel growth is inhibited. On P12, these pups are returned to room air, during which relative hypoxia triggers both normal vessel regrowth in the central retina and pathological peripheral retinal neovascularization, named as preretinal tufts, peaking at P17.[40,41] Thus, the P17 mouse retinas were subjected to the whole-mount retinal staining with the endothelial marker isolectin B4 (IB4). The results showed that there was a dramatic decrease in preretinal tufts from mice injected with rAAV1-dCasX/sgRNA-mPK5 than those with rAAV1-dCasX/sgRNA-*lacZ* in this OIR model without impacting growth of central new vessels (Figures 5A–5E).

In addition, qPCR and western blot analyses of the P17 mouse retinal tissues showed that there was significantly less *Pik3cd* mRNA and protein p110δ, as well as phosphorylated Akt in the retinas injected with rAAV1-dCasX/sgRNA-mPK5 than those injected with control rAAV1 in this OIR model (Figures 6A–6C). Inhibition of p110δ suppresses hypoxia-induced Akt activation and VEGF production.[31] Thereby, we examined vitreal VEGF levels by ELISA in those injected

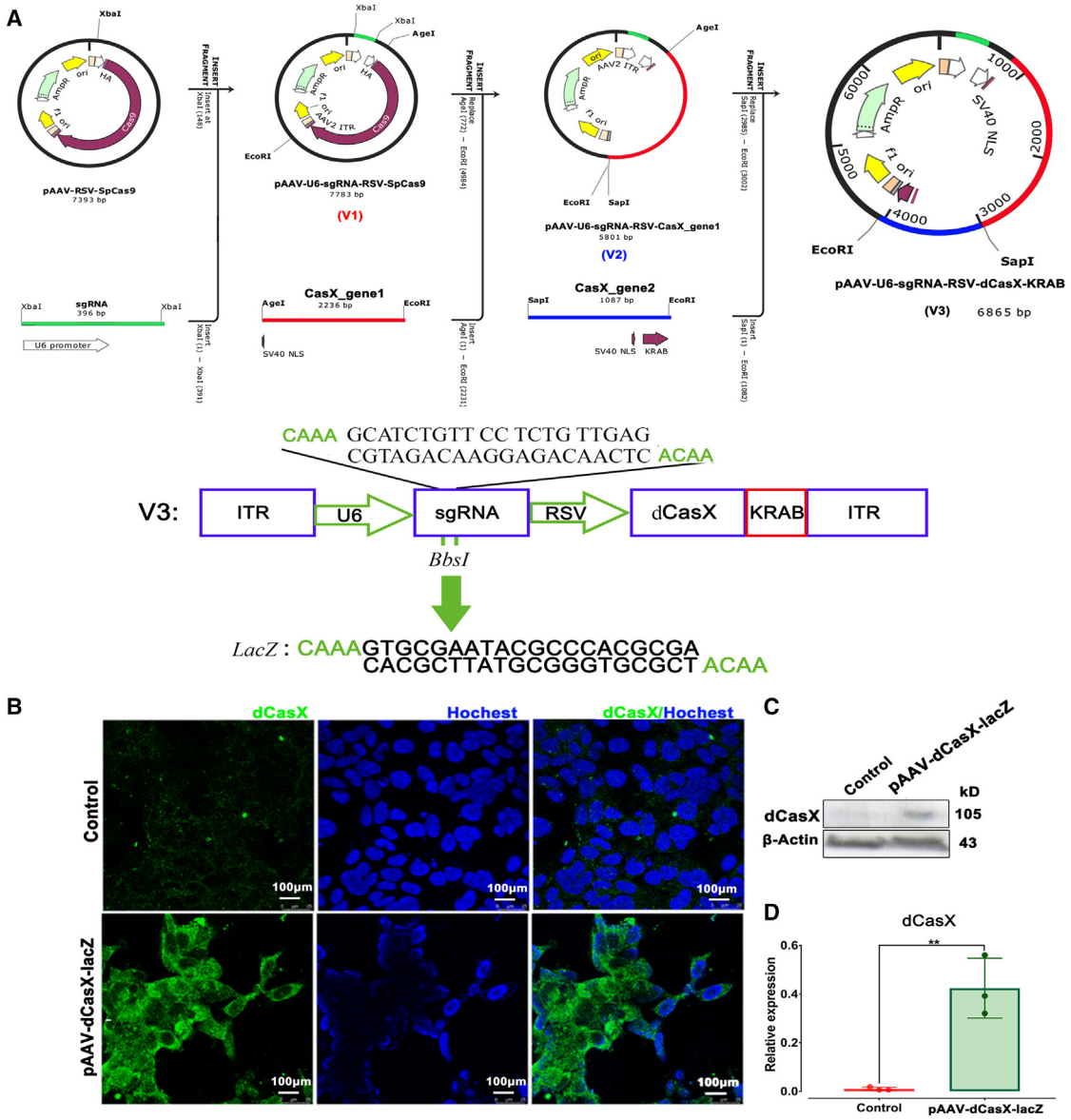

Figure 1. Establishment of an AAV vector expressing CRISPR/dCasX-KRAB

(A) Schematic diagram of constructing an AAV-CRISPR/dCasX-KRAB (dCasX) vector. The pAAV-U6-sgRNA/RSV-SpCas9 (V1) vector was originated from pAAV-RSV-SpCas9 (Addgene, 85450). The pAAV-U6-sgRNA/RSV-CasX_gene1 (V2) was derived from V1 by replacement of the Cas9 with CasX_gene1. The pAAV-U6-sgRNA/RSV-dCasX (V3) was originated from V2. ITR, inverted terminal repeat; U6, a promoter of polymerase III; RSV, a promoter of RSV.[52] (B) HEK293T cells were transfected with the plasmid of pAAV-dCasX/sgRNA-*lacZ*. 48 h later, the transfected cells were immunostained with a primary antibody against CasX. Green signals indicate dCasX expression. Scale bar, 100 μm. (C). Lysates of transfected HEK293T cells were subjected to Western blot analysis using indicated antibodies. A representative of at least three independent experiments is shown. (D) The bar graphs are mean ± SD of three independent experiments. The data was analyzed using one-way ANOVA followed by the Tukey honest significant difference *post hoc* test. **$p < 0.01$.

pups. The results showed that there was significantly less VEGF in the vitreous from the P17 mice injected with rAAV1-dCasX/sgRNA-mPK5 compared with those injected with control rAAV1 in this OIR model (Figure 6D). Collectively, these data show that suppression of p110δ with dCasX under the sgRNA-mPK5 guidance impedes hypoxia-induced Akt activation and VEGF production, resulting in a significant decrease in pathological retinal angiogenesis in this mouse model of OIR.

Notably, Intravitreal injection of rAAV1-dCasX/sgRNA-mPK5 into normal adult mice did not cause any detectable damage to the retina function and structure examined by electroretinography (ERG)

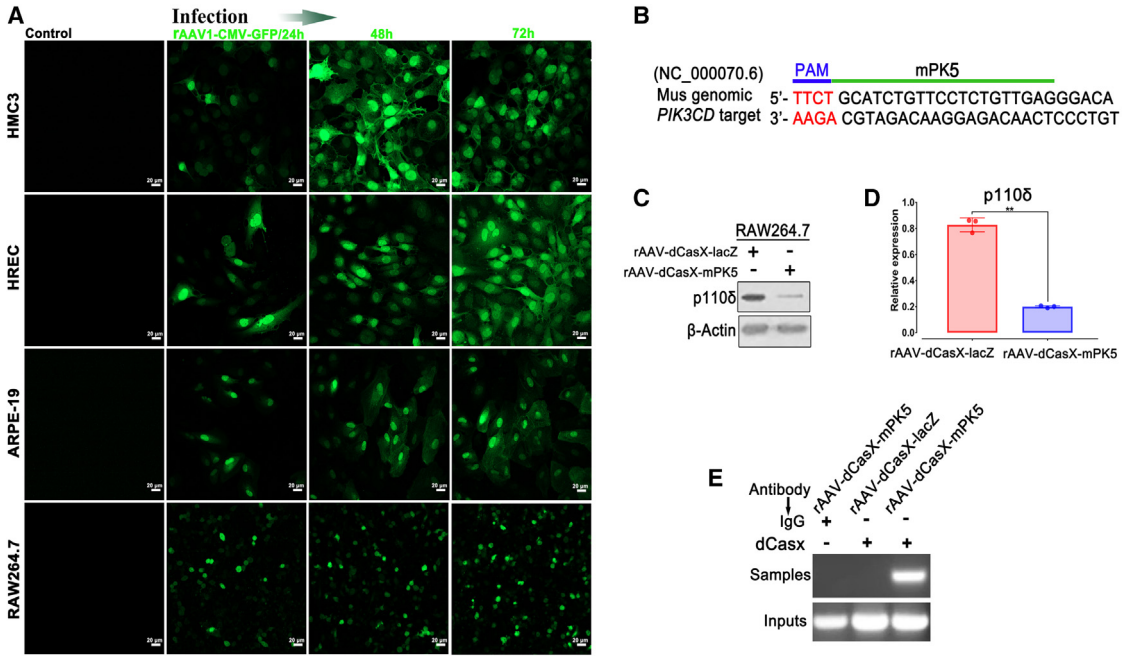

Figure 2. CRISPR/dCasX-KRAB-mediated blockage of p110δ expression *in vitro*

(A) HRECs, ARPE-19 cells and RAW264.7 were infected with rAAV1 virus carrying dCasX/sgRNA-*lacZ*. After 24, 48, and 72 h, the infected cells were immunostained with a primary antibody against dCasX. Green signals indicate dCasX expression. Scale bar, 20 μm. (B) Graphical schematic of a mouse *Pik3cd* locus. mPK5 sgRNA was originated from the *Pik3cd* promoter. The PAM is marked in blue. (C and D) Raw264.7 cells were infected with rAAV1-dCasX/sgRNA-*lacZ* and dCasX/sgRNA-mPK5, respectively. The transfected cells were subjected to western blotting analyses 48 h later (C and D). The bar graphs are mean ± SD of three independent experiments. The data was analyzed using one-way ANOVA followed by the Tukey honest significant difference *post hoc* test. **p < 0.01. (E) DNA samples from a ChIP assay with RAW264.7 cells, which were infected with rAAV1-dCasX/sgRNA-*lacZ* and dCasX/sgRNA-mPK5, respectively, were subjected to PCR and agarose gel electrophoresis analysis. Non-immune IgG served a negative control.[56]

(Figure S5), fluorescein fundus angiography (FFA) (Figure S6) and hematoxylin and eosin staining (Figure S7) at 4 weeks after intravitreal injection. All these data together suggest that the CRISPR/dCasX system can be leveraged for treating retinal neovascular diseases.

DISCUSSION

In this article, we report that a novel system of dCasX/sgRNA-mPK5 delivered with rAAV1 attenuates p110δ expression in the retina and prevents pathological retinal angiogenesis in a mouse model of OIR. Retinal neovascularization is a common pathological change in many diseases of the eye and has become an important cause of blindness.[42] Anti-VEGF drugs including ranibizumab and aflibercept are now a popular choice for treating intraocular neovascularization, but intravitreal anti-VEGF injections may contribute to fibrosis.[43] In addition, resistance to these drugs has been observed in many patients with PDR,[44] so the development of new therapeutic approaches to intraocular neovascularization is urgently needed. This novel system of rAAV1-dCasX/sgRNA-mPK5 we report here can be further developed as a potential alternative strategy for treating the angiogenesis-related eye diseases.

AAV does not cause any physiological or pathological changes after infecting the human body,[45] and it is the safest viral vector for gene therapy.[46–51] Nevertheless, the total packaging capacity of AAV is only 4.7 kb. In this study, we developed a new AAV-CRISPR/dCasX system by taking advantage of CasX being a small endonuclease with gene editing ability. In this study, we found that the intravitreally injected dCasX preferred to infect neovascular tufts to normal vascular ECs in the mouse model of OIR (Figures 4A–4E); this preferential transduction of tufts may be due to the fact that the neovessels are less mature than normal vessels and have an incomplete basement membrane and weaker intercellular junctions,[41] or that these tufts express a specific receptor for rAAV1. This warrants further investigation. The findings reported herein together suggest that rAAV1-medicated CRISPR/dCasX provides a new possibility for treating pathological retinal angiogenesis.

MATERIALS AND METHODS

Major reagents

Primary antibodies against p110δ, β-actin, Akt, and p-Akt were purchased from Cell Signaling Technology (Danvers, MA), and an antibody against dCasX was ordered from Hangzhou Huaan Biotechnology Co., Ltd (Hangzhou, Zhejiang, China). Alexa fluorescence-488-conjugated anti-CD11β antibody was purchased from Abcam (Cambridge, UK), Alexa fluorescence-532-conjugated anti-Panck antibody was from Nanostring (Nanostring Technologies, Seattle, WA), and

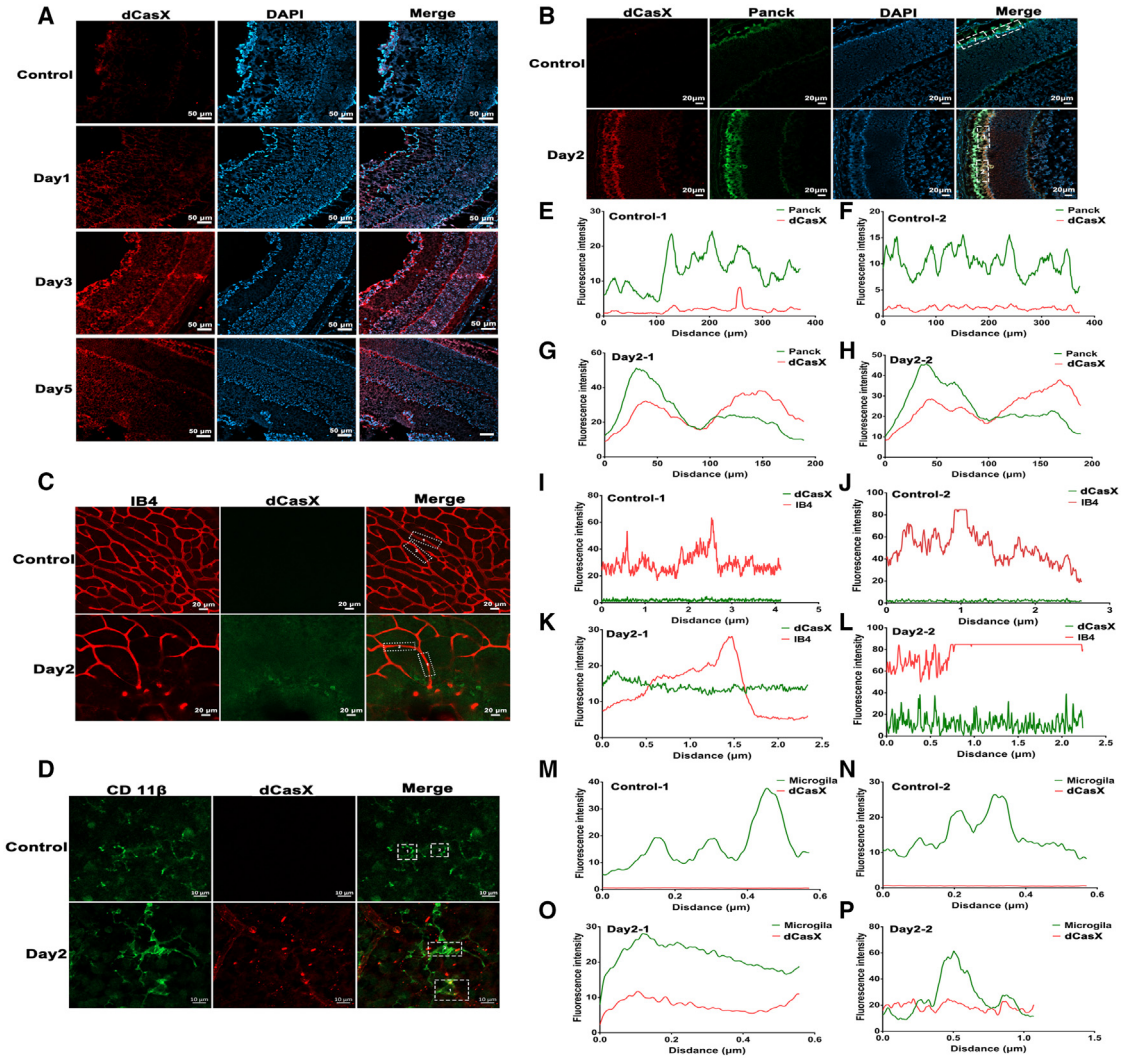

Figure 3. rAAV1-delivered dCasX expression *in vivo*

(A and B) Normal P12 mice were injected intravitreally with rAAV1 carrying dCasX/sgRNA-*lacZ* (1μL, 1.62 × 10E13 vg/mL). After injection for 1, 3, and 5 days, frozen eyeball sections were stained with a primary antibody against dCasX. Red signals indicate dCasX expression, and green indicate Panck expression. Scale bar, 20 μm. (C and D) Whole-mount retinas from the intravitreally injected in mice were stained with IB4 (red) and antibodies against dCasX and CD11β (green) and then with a fluorescent-labeled secondary antibody. Images were obtained in the immunofluorescence confocal microscope. Scale bars, 10 or 20 μm. (E–P) Co-localization analysis of dCasX expression *in vivo* was performed by ImageJ.[58] Two regions were selected for each image.

Alexa fluorescence-594-conjugated mouse endothelial-specific IB4 was purchased from Life Technology (Grand Island, NY). Alexa fluorescence-488-conjugated mouse anti-rabbit IgG and Alexa fluorescence-594-conjugated mouse anti-rabbit IgG were ordered from Hangzhou Huaan Biotechnology Co., Ltd. Horseradish peroxidase-conjugated mouse anti-rabbit IgG and goat anti-mouse IgG were purchased from Santa Cruz Biotechnology (Dallas, TX). Enhanced chemiluminescent substrate to detect horseradish peroxidase was purchased from Thermo Scientific (Waltham, MA). The plasmid of pAAV-RSV-SpCas9 was from our own laboratory deposited to Addgene (Cat. 85450, Cambridge, MA).[52] High-fidelity Herculase II DNA polymerases were from Agilent Technologies (Santa Clara, CA).

Cell culture

ARPE-19 cells (American Type Culture Collection [ATCC], Manassas, VA) were cultured in DMEM/F-12 (Invitrogen, Waltham, MA) supplemented with 10% fetal bovine serum. HRECs were purchased from Cell Systems (Kirkland, WA) and cultured in endothelial growth medium-2 (Lonza, Walkersville, MD). C57BL/6 mouse primary brain microvascular ECs (MVECs) were purchased from CellBiologics (Chicago, IL) and cultured in the EC medium with a kit (CellBiologics). HEK293 and 293T cells (HEK293, containing SV40 T-antigen) and RAW264.7 cells were purchased from ATCC and were cultured in DMEM with 10% fetal bovine serum. All cells were cultured at 37°C in a humidified 5% CO_2 atmosphere.[31,35]

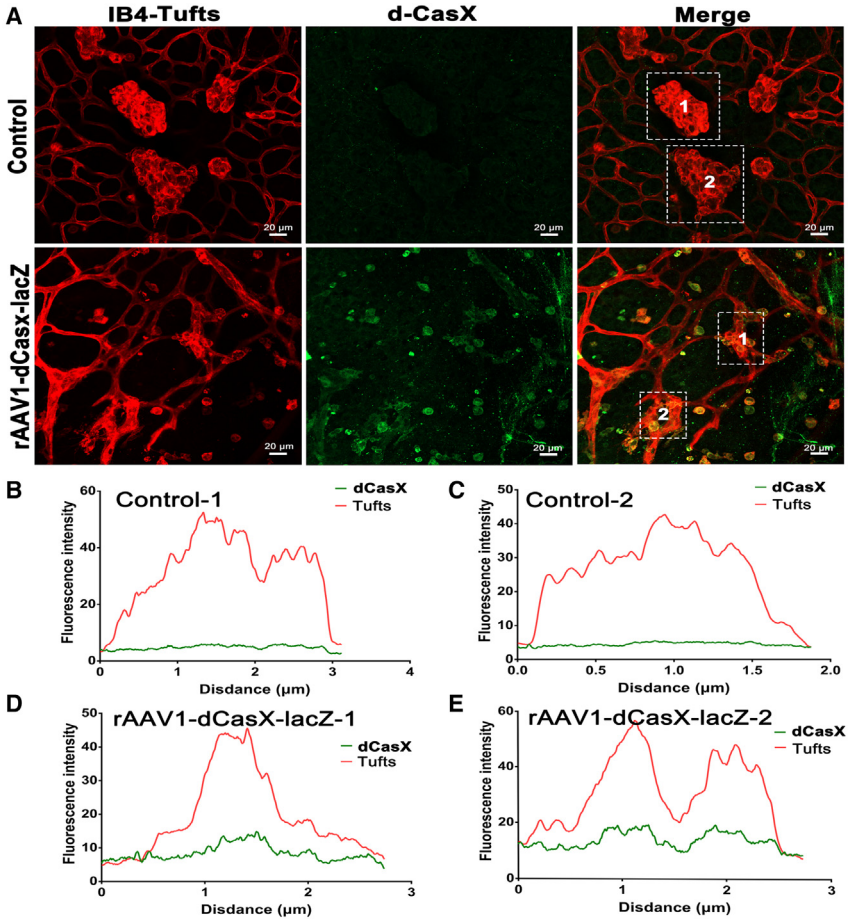

Figure 4. rAAV1 infects pathological vascular ECs with high efficiency

(A) P12 mice that had been exposed to 75% oxygen for 5 days were injected intravitreally with rAAV1-dCasX/sgRNA-*lacZ* (1μL, 1.62 × 10E13 vg/mL). Whole-mount retinas from the P17 mice in a model of OIR were stained with IB4 (red) and a primary antibody against dCasX and then a fluorescent-labeled secondary antibody. Scale bar, 20 μm. (B–E) Co-localization analysis of dCasx expression with tufts *in vivo* was performed by ImageJ.[41] Two regions were selected for each image.

Mice

Six-week-old C57BL/6J mice were purchased from Institute of Basic Medicine and Cancer, Chinese Academy of Sciences (Hangzhou) and used for breeding to generate pups. All the animal experiments followed the guideline of the Association for Research in Vision and Ophthalmology Statement for the Use of Animals in Ophthalmic and Vision Research. All the mice were cared for by following the protocol approved by the Institutional Animal Care at Institute of Basic Medicine and Cancer (Hangzhou, China).[31]

DNA constructs

The 20-nt target DNA sequences (5′-GCATCTGTTCCTCTGTTGAG-3′, mPK5) preceding a 5′-TTCN PAM sequence at -exon 2 in the promoter of mouse genomic *Pik3cd* locus was selected for generating sgRNA for CasX targets. The control sgRNA sequence (5′-TGCGAATACGCCCACGCGAT-3′) was designed to target the *lacZ* gene from *Escherichia coli*. The pAAV-RSV-dCasX/U6-sgRNA vector was originated from pAAV-RSV-SpCas9 (Addgene, 85450). Briefly, the pAAV-U6-sgRNA/RSV-SpCas9 (V1) vector was originated from pAAV-RSV-SpCas9 (Addgene, 85450) by inserting fragment U6-sgRNA (396 bp) at *Xba*I site (148 bp) with T4 ligation. The 396-bp U6-sgRNA was PCR amplified from pBLO 62.4 vector (Addgene, 123123) by primers U6-sgRNA forward (5′CGGCCTCTAGAGAGGGCCTATTTCCCATGAT3′) and U6-sgRNA reverse (5′ACATTTCTAGACAAAAAACAGTGTCTTC3′). Then, the pAAV-U6-sgRNA/RSV-CasX_gene1 (V2) was derived from V1 by replacement of the Cas9 using AgeI/EcoRI with CasX_gene1, which was PCR amplified CasX (Met1 to Gly730) from pBLO 62.4 vector. The PCR primers for this amplification were CasX_gene1 forward (5′ATAAAACCGGTGCCACCATGGCCCCAAAGAAGAAGCG 3′) and CasX_gene1 reverse (5′ACTACGAATTCAGCATGCTCTTCTCTGTTCCAC3′). The pAAV-U6-sgRNA/RSV-dCasX (V3) was originated from V2 by inserting fragment dCasX_gene2 with KRAB (1087 bp) at *Sap*I/*Eco*RI with T4 ligation. The dCasX fragment in the dCasx_gene2 was synthesis based on the pBLO 62.4 vector with the mutation at Asp672Ala, Glu769Ala and Asp935Ala. The *KRAB* gene fused with dCasX_gene2 was the same as fused with dCas9 (Addgene, 110820) from 4852 bp to 5139 bp. All these constructs were confirmed by DNA sequencing.[52]

To construct the SpGuide targeting the promoter of mouse *Pik3cd*, the top oligo: 5′-CAAAGCATCTGTTCCTCTGTTGAG-3′ and bottom oligo: 5′-AACACTCAAC AGAGGAACAGATGC-3′ were annealed and cloned into the V3 vector by *BbsI*. All clones were confirmed by DNA sequencing using a primer 5′-GGACTATCAT ATGCTTACCG-3′ from the sequence of U6 promoter, which drives expression of sgRNAs.[35]

Both synthesis of primers and oligos and sequencing of PCR products and clones were done by Massachusetts General Hospital DNA Core Facility (Cambridge, MA).

AAV production and transduction

The recombinant viruses of rAAV2/1 were produced by Weizhen Biotechnology (Jinan, Shandong, China) as described previously.[53] Briefly, transfection of AAV package plasmid (AAV2/1), transgene plasmid (pAAV-RSV-dCasX/sgRNA-mPK5 or pAAV- RSV-dCasX/sgRNA-*lacZ*) and adenovirus helper plasmid were performed in a

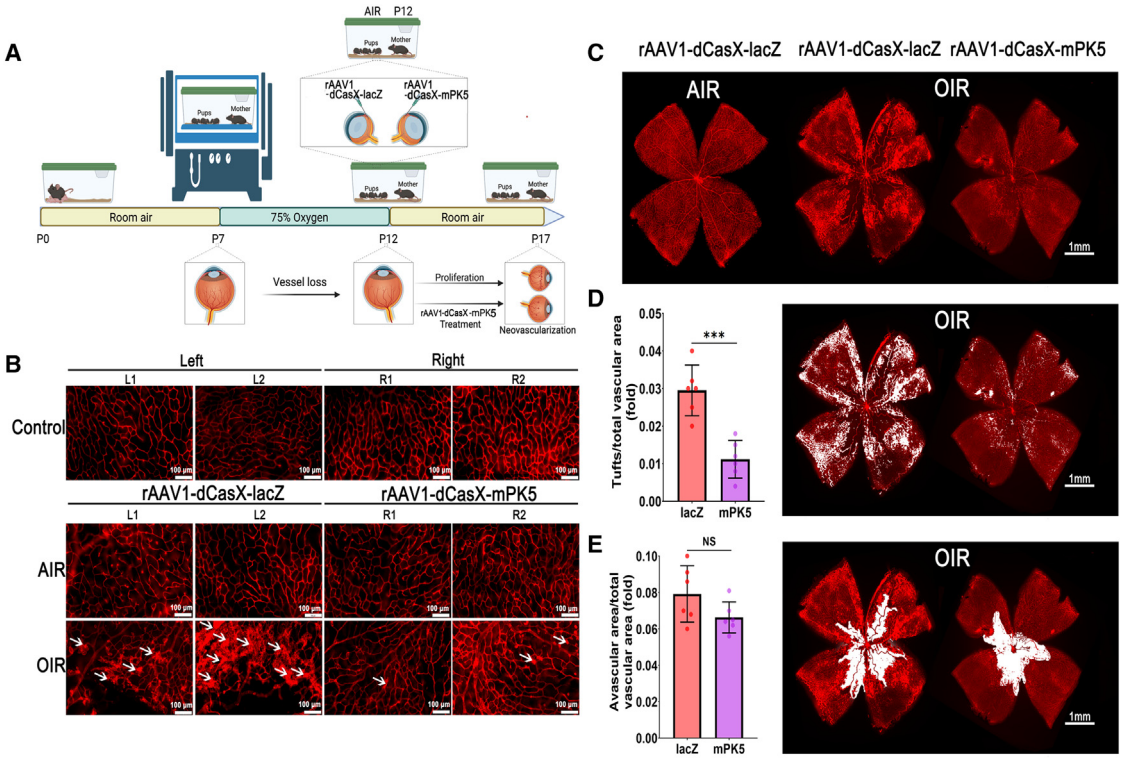

Figure 5. CRISPR/dCasX-KRAB-mediated blockade of p110δ expression suppresses pathological angiogenesis in a mouse model of OIR

(A) Schematic graph of the OIR model. Litters of P12 mice that had been exposed to 75% oxygen for 5 days were injected intravitreally with rAAV1 (1 μL, 1.62 × 10E13 vg/mL) carrying dCasX/sgRNA-*lacZ* or dCasX/sgRNA-mPK5.[41] (B) The whole-mount retinas from the injected P17 mice were stained with IB4. Arrows indicate tufts. AIR indicates mice that were kept in room air without exposure to 70% oxygen. L, left eye of the mice; R, right eye of the mice. Scale bar, 100 μm. (C–E) Quantification of tufts and avascular areas as described previously.[40] The bar graphs are mean ± SD (n = 6). The data were analyzed using one-way ANOVA followed by the Tukey honest significant difference *post hoc* test. ***p < 0.01. NS, not significant.

10-layer hyper flask containing confluent HEK 293 cells. At day 3 after transfection, the cells and culture medium were collected and enzymatically treated with Benzonase (EMD Millipore, Burlington, MA). After high-speed centrifugation and filtration, the cell debris was cleared. The clarified viral solution was loaded onto an iodixanol gradient column. After ultracentrifugation, the pure vectors were separated and extracted, and then run through an Amicon Ultra-Centrifugal Filter device (EMD Millipore) for desalting. Both vectors were titrated by TaqMan PCR amplification (Applied Biosystems 7500, Life Technologies), with the primers and probes detecting the transgene and ITR. SDS-PAGE was performed to check the purity of the vectors, which were named AAV1- dCasX/sgRNA-mPK5 (1.62 × 10E13 vg/mL), and AAV1-dCasX/sgRNA-*lacZ* (1.81 × 10E13 vg/mL).

HRECs, ARPE-19, and RAW264.7 cells grown to 50% confluence in 48-well plates were changed into the fresh cultured media before adding either with rAAV1-dCasX/sgRNA-*lacZ*, rAAV1-dCasX/sgRNA-mPK5, or rAAV1-CMV-GFP (Weizhen Biotechnology) (1.62 × 10E13 vg/mL, 2 μL/well) into each well. The cells were photographed under an immunofluorescence microscope for determining the rAAV1 transduction efficiency post 6, 24, 48 and 72 h.

In addition, the plasmid of pAAV-RSV-dCasX/sgRNA-*lacZ* was mixed with Lipofectamine 3000 (Thermo Fisher Scientific) along with Opti-MEM (Thermo Fisher Scientific). This transfection mixture was kept at room temperature for 30 min and then added dropwise into HEK-293T cells in a six-well plate. At 72 h after transfection, the cells were subjected to immunofluorescence or western blot analysis.[31,35]

Western blotting

Detailed protocols were described in our previous report.[54] Briefly, cells or retinas were lysed in a 1× sample buffer that was diluted with extraction buffer (10 mM Tris-HCl, pH 7.4, 5 mM EDTA, 50 mM NaCl, 50 mM NaF, 1% Triton X-100, 20 μg/mL aprotinin, 2 mM Na_3VO_4, and 1 mM phenylmethylsulfonyl fluoride) from 5× protein sample buffer (25 mM EDTA [pH 7.0], 10% SDS [Sigma-Aldrich, St. Louis, MO], 500 mM dithiothreitol, 50% sucrose, 500 mM Tris.HCl [pH 6.8], and 0.5% bromophenol blue). Then, samples were boiled for 5–8 min, and centrifuged them for 5 min at 13,000×*g*. Subsequently, proteins in samples were separated by 10% SDS-PAGE, transferred to polyvinylidene difluoride membranes, and subjected to western blot analyses. Experiments were repeated at least three

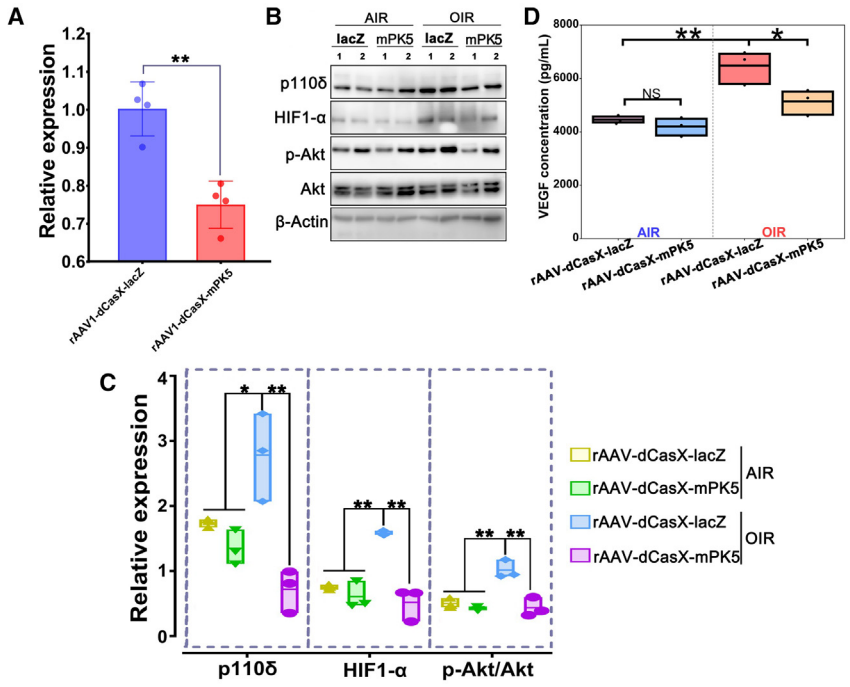

Figure 6. dCasX-mediated p110δ attenuation suppresses Akt activation and VEGF production in the mouse model of OIR

(A and B) Retinal mRNA and proteins from P17 mice (n = 6) subjected to qPCR (A) and western blotting analyses with indicated antibodies (B), respectively. (C) The intensity of bands. The bar graphs are mean ± SD of three independent experiments. The data were analyzed using one-way ANOVA followed by the Tukey honest significant difference (HSD) *post hoc* test. *p < 0.05, **p < 0.01. (D) Clarified vitreous (5 μL) from the P17 mice with or without experiencing OIR was subjected to ELISA analysis by following the instructions of a Quantikine Mouse VEGF ELISA Kit.[31] The bar graphs are mean ± SD of six mice. The data were analyzed using one-way ANOVA followed by the Tukey HSD *post hoc* test. NS, not significant. *p < 0.05; **p < 0.01.

times. Signal intensity was determined by densitometry with ImageJ software.

Immunofluorescence

This experiment was performed as described previously.[54] Briefly, cultured cells or frozen section of eyeballs were fixed in 3.7% formaldehyde/phosphate-buffered saline (PBS) for 10 min at room temperature. They were then blocked with 5% normal goat serum in 0.3% Triton X-100/PBS for 30 min and incubated with primary antibodies (1:200 dilution) overnight at 4°C. After thorough washes with 0.3% Triton X-100/PBS, samples were incubated with fluorescent-labeled secondary antibodies (1:300 dilution in a blocking buffer) for 1 h. Finally, samples were washed with 0.3% Triton X-100/PBS, mounted in a mount medium with 4′, 6-diamidino-2-phenylindole (Vector Laboratories, Newark, CA). Photographs were taken in a confocal microscope (ZEISS 900).

qPCR

The total RNA of RAW264.7 cells and retina tissues treated by rAAV1-dCasX/sgRNA-mPK5 or *lacZ* was extracted using the RNeasy Plus Mini Kit (Qiagen, Germantown, MD). Primers of quantitative PCR synthesized by Integrated DNA Technology (Coralville, IA) were forward: 5′-TTTGGAATCAACCGAGAGCG-3′, reverse: 5′-TTTAGGGATATCTGGGTTCT-3′ for mouse *Pik3cd* and forward: 5′-ACTCAGGAGAGTGTTTCCTCG-3′, reverse: 5′-TTTGCCGTGAGTGGAGTCAT-3′, for the housekeeping gene *GADPH*.[37]

RNA sequencing

MVECs at 70%–80% confluence in six-well plates were treated with rAAV1-sgRNA-*lacZ* and rAAV1-dCasX-sgRNA-*lacZ* (10 μL/well, 1.81 × 10E13 vg/mL) for 72 h. The treated cells were then harvested by Trizol for RNA isolation using an OMEGA kit (R6834). Subsequently, a cDNA library was established and the quality and integrity of the RNA was examined by a Nano drop analysis. RNA sequencing was performed by NovaSeq 6000. The differential genes were screened to satisfy $|\log2FC| \geq 1$ and $p < 0.05$, and genes were further screened to identify significantly differentially expressed genes as described previously.[55]

Bioinformatics data analysis

RNA sequencing data were subjected to| log2FC | 1 or higher and $p < 0.05$ Gene Ontology (GO) enrichment analysis as well as Kyoto Encyclopedia of Genes and Genomes (KEGG) pathway enrichment analysis on the differentially expressed genes. More specifically, we analyzed GO and KEGG enrichment on the differentially expressed genes for their functions, mapped differentially expressed genes to each term of the GO database, counted the number of genes in each term, and then used a hypergeometric distribution test to obtain significantly enriched GO terms and KEGG pathways for the differently expressed genes and for the differentially expressed genes based on the KEGG annotations of the entire genome, respectively.[55]

ChIP and DNA sequencing

In brief,[56] the cross-link of protein-DNA complexes was performed by adding 37% paraformaldehyde (PFA) diluted to a 1% final concentration and cells were incubated at room temperature for 15 min. Glycine (125 mM) was applied for quenching the fixation. Five hundred microliters lysis buffer (10 μg/mL leupeptin, 10 μg/mL aprotinin, and 1 mM phenylmethylsulfonyl fluoride) was added per 5×10^6 cells for resuspension. Cell lysates were sonicated to shear chromatin to an average length of approximately 1 kb. After being centrifuged at 12,000×*g*, the supernatant was collected. Agarose beads were incubated with 5 μg anti-dCasX and anti-IgG primary antibody at 4°C on a rotating device for 2 h for a better combination. Then the prepared samples were added to the beads and incubated at

4°C overnight. The following day, beads were collected after centrifugation and washed four times. One hundred microliters Tris-EDTA buffer was added to the sample and boiled for 10 min. Finally, samples were centrifuged for 1 min at 12,000×*g* and supernatant were collected into a clean tube. The ChIP samples were amplified by PCR with the primers and subjected to gel analysis,[56] and the PCR products purified from the gel were subjected to Sanger DNA sequencing. Primers for CasX guided by mPK5 binding to the promoter of mouse *Pik3cd* were P59F: 5′-TGTGATTGGGTTACTTC ACT-3′, P59R: 5′- AGCAATGGGAGATAATAGCC-3′, and primers for CasX binding to potential offtagets (PO1: atctgttcct ctgttgag at *Mus musculus* chromosome 16 from 4085896-4085913) guided by mPK5 were PO1F: 5′-gggatattttctagttccct-3′, PO1R: 5′-catgtaataagg acgcatgc-3′, and (PO2: ctcaacagag gaacagat at *Mus musculus* chromosome 16 from 80912676 to 80912676) PO2F: tataacactc ctgggcatat, PO2R: ggatatttctagctccatgg.

A mouse model of OIR

This mouse OIR model was performed according to previous publications.[35,41] C57BL/6J litters on P7 were exposed to 75% oxygen until P12 in the oxygen chamber. Oxygen concentration was monitored daily using an oxygen sensor. On P12, the pups were anesthetized by intraperitoneal injection of 10 mL/kg 1% pentobarbital sodium. During intravitreal injections, eyelids of P12 pups were separated by incision. Intravitreous injections were performed under a microsurgical microscope using glass pipettes with a diameter of approximately 150 μm at the tip after the eye were punctured at the upper nasal limbus using a BD insulin syringe with the BD ultra-fine needle. rAAV1-CasX/sgRNA-*lacZ* or rAAV1-dCasX/sgRNA-mPK5 (1 μL, 1.62 × 10E13 vg/mL) was intravitreally injected. After injection, the eyes were treated with a triple antibiotic (*Neo*/Poly/Bac) ointment and kept in room air (21% oxygen). On P17, the mice were sacrificed and retinas were carefully removed and fixed in 3.7% PFA. Mice weighing less than 6 g were excluded from the experiments. In total, there were three experiments performed in this OIR model. Retinal whole mounts were stained overnight at 4°C with murine specific vascular ECs marker IB4-Alexa 594 (red). The images were taken with an automatic tissue scanning machine (Olympus VS200).

Quantification of pathological retinal vessels

This quantification was performed as described previously.[40] Briefly, retinal image was imported into Adobe Photoshop CS4, and the Polygonal Lasso tool was used to trace the vascular area of the entire retina. Once the vascular area was highlighted, the number of pixels was obtained. After selecting total retinal area, the Lasso tool and the "subtract from selection" icon was used to selectively remove the vascularized retina, leaving behind only the avascular area. Once the avascular region was selected, click the refresh icon again to obtain the number of pixels in the avascular area.[31]

Enzyme-linked immunoassay

This assay was conducted by following the instructions of a Quantikine Mouse VEGF ELISA Kit (Cat.MMV00; R&D Systems). Briefly, clarified vitreous (5 μL) from each eye from P17 mice with or without experiencing OIR was diluted with PBS to 50 μL, which was added into each well. In addition, 50 μL standard was added to each well, and incubated at room temperature for 2 h. Then, after the wells were washed with wash buffer for five times, 100 μL conjugate from the kit was added to each well and incubated at room temperature for 2 h. After wash for five times, 100 μL substrate solution was added to each well and incubated for 30 min. Then, 100 μL of stop solution was added into each well. Finally, the plate was read at 450 nm within 30 min.[57]

ERG

Five 20-day-old mice were anesthetized and each underwent an intravitreal injection with 1 μL rAAV1-dCasX-KRAB/sgRNA-mPK5 as described above. After 2 weeks, ERG (by dark adaptation, using a DIAGNOSYS Celeris containing an interior stimulator) was performed as followed. After overnight dark adaptation, the animals were prepared for ERG recording under dim red light. While under anesthesia with a mixture of ketamine 1% pentobarbital sodium (10 mg/kg i.p.), their pupils were dilated using one drop of 1% tropicamide followed by one drop of 1% cyclopentolate hydrochloride applied on the corneal surface. One drop of Genteal (corneal lubricant) was applied to the cornea of the untreated eye to prevent dehydratation. A drop of 0.9% sterile saline was applied on the cornea of the treated eye to prevent dehydration and to allow electrical contact with the recording electrode. The binocular stimulators were aimed at both eyes of the mouse, and the impedance was less than 10 Ω. A series of flash intensities was produced by the stimulators to test both scotopic and photopic response.[41]

FFA

The following day after ERG, FFA was performed on the mice. Animals were anesthetized a mixture of ketamine 1% Pentobarbital sodium (10 mg/kg intraperitoneal injection), their pupils were dilated using a drop of 1% tropicamide followed by one drop of 1% cyclopentolate hydrochloride applied on the corneal surface. One drop of sterile saline was placed on the experimental eye to remove any debris followed by Genteal. Genteal was placed on both eyes to prevent corneal drying. Then, 0.01 mL 25% sodium fluorescein (pharmaceutical grade sodium fluorescein; Akorn, Lake Forest, IL) 5 g body weight was injected through a peritoneal route. Photos were taken sequentially at 1, 2, and 3 min after fluorescein injection. A Micron III (Phoenix Research Industries, Duluth, GA) system was used for taking fundus photographs according to the manufacturer's instructions. The mice were placed in front of the fundus camera and pictures of the retina taken for monitoring retinal function.[41]

Statistics

Data were analyzed as described preciously.[54] At least three independent experiments were analyzed using an unpaired t test between two groups and ordinary one-way ANOVA followed by the Tukey honest significant difference *post hoc* test. For animal experiments, the data from at least six mice were used for the statistical analysis. A p value of less than 0.05 was considered significantly difference. All relevant data are available from the authors.[41]

DATA AND CODE AVAILABILITY

The materials described in this report, including all relevant raw data, will be freely available to any researcher wishing to use for noncommercial purposes, without breaching participant confidentiality.

SUPPLEMENTAL INFORMATION

Supplemental information can be found online at https://doi.org/10.1016/j.omtn.2023.08.001.

ACKNOWLEDGMENTS

This research was supported by National Natural Science Foundation of China (82070989) to H.L., Introduction Plan of High-Level Foreign Experts (G2022026027L) to H.L. and G.M., Major Program of Medical Science Challenging Plan of Henan province (SBGJ202102190) to G.M., China Scholarship Council (201806320148) to H.H., Research Projects for Social Development of Ningxia [No.2021BEG03072] to Y.Y. No funding bodies had any role in study design, data collection and analysis, decision to publish, or preparation of the manuscript.

AUTHOR CONTRIBUTION

H.H., Y.Y., and Y.J. performed most of the experiments, analyzed the results and wrote the manuscript; H.Q., Z.H., L.W., and L.D. performed some of the experiments; J.T., B.V., X.L., and J.L. revised the manuscript; G.M. and H.L. conceived the experiments, analyzed the data and revised the manuscript.

DECLARATION OF INTERESTS

All the authors declare that they have no conflicts of interest with the contents of this article.

REFERENCES

1. Šuleková, M., and Fitzgerald, K.T. (2019). Can the Thought of Teilhard de Chardin Carry Us Past Current Contentious Discussions of Gene Editing Technologies? Camb. Q. Healthc. Ethics *28*, 62–75.
2. Gasiunas, G., Sinkunas, T., and Siksnys, V. (2014). Molecular mechanisms of CRISPR-mediated microbial immunity. Cell. Mol. Life Sci. *71*, 449–465.
3. Wagner, J.C., Platt, R.J., Goldfless, S.J., Zhang, F., and Niles, J.C. (2014). Efficient CRISPR/Cas9-mediated genome editing in P. falciparum. Nat. Methods *11*, 915–918.
4. Gu, P., Yang, Q., Chen, B., Bie, Y.N., and Gu, W. (2021). Genetically blocking HPD via CRISPR/Cas9 protects against lethal liver injury in a pig model of tyrosinemia type I. Mol. Ther. Methods Clin. Dev. *21*, 530–547.
5. Shinmyo, Y., Tanaka, S., Tsunoda, S., Hosomichi, K., Tajima, A., and Kawasaki, H. (2016). CRISPR/Cas9-mediated gene knockout in the mouse brain using *in utero* electroporation. Sci. Rep. *6*, 20611.
6. Qin, W., Dion, S.L., Kutny, P.M., Zhang, Y., Cheng, A.W., Jillette, N.L., Malhotra, A., Geurts, A.M., Chen, Y.G., and Wang, H. (2015). Efficient CRISPR/Cas9-Mediated Genome Editing in Mice by Zygote Electroporation of Nuclease. Genetics *200*, 423–430.
7. Tan, Y., Ye, L., Kan, Y., Wai, X., and Fei, W. (2016). Genome editing using CRISPR-Cas9 to create the HPFH genotype in HSPCs: An approach for treating sickle cell disease and beta-thalassemia. Proc. Natl. Acad. Sci. USA *113*, 10661–10665.
8. Yin, H., Xue, W., Chen, S., Bogorad, R.L., Benedetti, E., Grompe, M., Koteliansky, V., Sharp, P.A., Jacks, T., and Anderson, D.G. (2014). Genome editing with Cas9 in adult mice corrects a disease mutation and phenotype. Nat. Biotechnol. *32*, 551–553.
9. Seeger, C., and Sohn, J.A. (2014). Targeting Hepatitis B Virus With CRISPR/Cas9. Mol. Ther. Nucleic Acids *3*, e216.
10. Horvath, P., and Barrangou, R. (2010). CRISPR/Cas, the Immune System of Bacteria and Archaea. Science *327*, 167–170.
11. Zhang, Y., and Karakikes, I. (2021). Translating Genomic Insights into Cardiovascular Medicines: Opportunities and Challenges of CRISPR-Cas9. Trends Cardiovasc. Med. *31*, 341–348.
12. Søndergaard, J.N., Geng, K., Sommerauer, C., Atanasoai, I., Yin, X., and Kutter, C. (2020). Successful delivery of large-size CRISPR/Cas9 vectors in hard-to-transfect human cells using small plasmids. Commun. Biol. *3*, 319.
13. Picard, M. (2022). Why do we care more about disease than health? Phenomics *2*, 145–155.
14. Zhang, H., Hua, X., and Song, J. (2021). Phenotypes of Cardiovascular Diseases: Current Status and Future Perspectives. Phenomics *1*, 229–241.
15. Yan, Z., Sun, X., and Engelhardt, J.F. (2009). Progress and prospects: techniques for site-directed mutagenesis in animal models. Gene Ther. *16*, 581–588.
16. Xie, Q., Bu, W., Bhatia, S., Hare, J., Somasundaram, T., Azzi, A., and Chapman, M.S. (2002). The atomic structure of adeno-associated virus (AAV-2), a vector for human gene therapy. Proc. Natl. Acad. Sci. USA *99*, 10405–10410.
17. Burstein, D., Harrington, L.B., Strutt, S.C., Probst, A.J., Anantharaman, K., Thomas, B.C., Doudna, J.A., and Banfield, J.F. (2017). New CRISPR-Cas systems from uncultivated microbes. Nature *542*, 237–241.
18. Okano, K., Sato, Y., Hizume, T., and Honda, K. (2021). Genome editing by miniature CRISPR/Cas12f1 enzyme in Escherichia coli. J. Biosci. Bioeng. *132*, 120–124.
19. Kaya, M., and Endo, T. (2016). Highly specific targeted mutagenesis in plants using Staphylococcus aureus Cas9. Sci. Rep-UK *2016*, 6.
20. Hsu, P.D., Lander, E.S., and Zhang, F. (2014). Development and Applications of CRISPR-Cas9 for Genome Engineering. Cell *157*, 1262–1278.
21. Isner, J.M., and Asahara, T. (1999). Angiogenesis and vasculogenesis as therapeutic strategies for postnatal neovascularization. J. Clin. Invest. *103*, 1231–1236.
22. Takagi, H., Koyama, S., Seike, H., Oh, H., Otani, A., Matsumura, M., and Honda, Y. (2003). Potential Role of the Angiopoietin/Tie2 System in Ischemia-Induced Retinal Neovascularization. Invest. Ophthalmol. Vis. Sci. *44*, 393–402.
23. Perrotta, P., Van der Veken, B., Van Der Veken, P., Pintelon, I., Roosens, L., Adriaenssens, E., Timmerman, V., Guns, P.J., De Meyer, G.R.Y., and Martinet, W. (2020). Partial Inhibition of Glycolysis Reduces Atherogenesis Independent of Intraplaque Neovascularization in Mice. Arteriosclerosis *40*, 1168–1181.
24. Adamis, A.P., Miller, J.W., Bernal, M.T., D'Amico, D.J., Folkman, J., Yeo, T.K., and Yeo, K.T. (1994). Increased Vascular Endothelial Growth Factor Levels in the Vitreous of Eyes With Proliferative Diabetic Retinopathy. Am. J. Ophthalmol. *118*, 445–450.
25. Wang, X., Wang, G., and Wang, Y. (2009). Intravitreous Vascular Endothelial Growth Factor and Hypoxia-Inducible Factor 1a in Patients With Proliferative Diabetic Retinopathy. Am. J. Ophthalmol. *148*, 883–889.
26. Yang, Y., Yang, K., Li, Y., Li, X., Sun, Q., Meng, H., Zeng, Y., Hu, Y., and Zhang, Y. (2013). Decursin inhibited proliferation and angiogenesis of endothelial cells to suppress diabetic retinopathy via VEGFR2. Mol. Cell. Endocrinol. *378*, 46–52.
27. Davis, M.D. (1965). Vitreous Contraction in Proliferative Diabetic Retinopathy. Arch. Ophthalmol. *74*, 741–751.
28. Bernaudin, M., Nedelec, A.S., Divoux, D., Mackenzie, E.T., Petit, E., and Schumann-Bard, P. (2002). Normobaric Hypoxia Induces Tolerance to Focal Permanent Cerebral Ischemia in Association with an Increased Expression of Hypoxia-Inducible Factor-1 and its Target Genes, Erythropoietin and VEGF, in the Adult Mouse Brain. J. Cerebr. Blood Flow Metabol. *22*, 393–403.
29. Do, J.Y., Choi, Y.K., Kook, H., Suk, K., Lee, I.K., and Park, D.H. (2015). Retinal hypoxia induces vascular endothelial growth factor through induction of estrogen-related receptor γ. Biochem. Biophys. Res. Commun. *460*, 457–463.
30. Bennis, Y., Sarlon-Bartoli, G., HUBERT, àL., Lucas, L., Pellegrini, L., Velly, L., Blot-Chabaud, M., Dignat-Georges, F., Sabatier, F., and Pisano, P. (2012). Priming of late endothelial progenitor cells with erythropoietin before transplantation requires the CD131 receptor subunit and enhances their angiogenic potential. J. Thromb. Haemostasis *10*, 1914–1928.

31. Wu, W., Zhou, G., Han, H., Huang, X., Jiang, H., Mukai, S., Kazlauskas, A., Cui, J., Matsubara, J.A., Vanhaesebroeck, B., et al. (2020). PI3Kδ as a Novel Therapeutic Target in Pathological Angiogenesis. Diabetes *69*, 736–748.

32. Parsi, K.M., Hennessy, E., Kearns, N., and Maehr, R. (2017). Using an Inducible CRISPR-dCas9-KRAB Effector System to Dissect Transcriptional Regulation in Human Embryonic Stem Cells (Springer New York).

33. Boulos, S., Meloni, B.P., Arthur, P.G., Bojarski, C., and Knuckey, N.W. (2006). Assessment of CMV, RSV and SYN1 promoters and the woodchuck post-transcriptional regulatory element in adenovirus vectors for transgene expression in cortical neuronal cultures. Brain Res. *1102*, 27–38.

34. Pan, X., Yue, Y., Zhang, K., Lostal, W., Shin, J.-H., and Duan, D. (2013). Long-term robust myocardial transduction of the dog heart from a peripheral vein by adeno-associated virus serotype-8. Hum. Gene Ther. *24*, 584–594.

35. Han, H., Chen, N., Huang, X., Ling, B., Tian, J., and Hetian, L. (2019). Correction: Phosphoinositide 3-kinase δ inactivation prevents vitreous-induced activation of AKT/MDM2/p53 and migration of retinal pigment epithelial cells. J. Biol. Chem. *294*, 18517.

36. Spilsbury, K., Garrett, K.L., Shen, W.Y., Constable, I.J., and Rakoczy, P.E. (2000). Overexpression of Vascular Endothelial Growth Factor (VEGF) in the Retinal Pigment Epithelium Leads to the Development of Choroidal Neovascularization. Am. J. Pathol. *157*, 135–144.

37. Wu, W.-K., Llewellyn, O.P.C., Bates, D.O., Nicholson, L.B., and Dick, A.D. (2011). IL-10 regulation of macrophage VEGF production is dependent on macrophage polarisation and hypoxia. Immunobiology.

38. Ellis, B.L., Hirsch, M.L., Barker, J.C., Connelly, J.P., Steininger, R.J., 3rd, and Porteus, M.H. (2013). A survey of *ex vivo*/*in vitro* transduction efficiency of mammalian primary cells and cell lines with Nine natural adeno-associated virus (AAV1-9) and one engineered adeno-associated virus serotype. Virol. J. *10*, 74.

39. Grieger, J.C., Choi, V.W., and Samulski, R.J. (2006). Production and characterization of adeno-associated viral vectors. Nat. Protoc. *1*, 1412–1428.

40. Connor, K.M., Krah, N.M., Dennison, R.J., Aderman, C.M., Chen, J., Guerin, K.I., Sapieha, P., Stahl, A., Willett, K.L., and Smith, L.E.H. (2009). Quantification of oxygen-induced retinopathy in the mouse: a model of vessel loss, vessel regrowth and pathological angiogenesis. Nat. Protoc. *4*, 1565–1573.

41. Huang, X., Zhou, G., Wu, W., Duan, Y., Ma, G., Song, J., Xiao, R., Vandenberghe, L., Zhang, F., D'Amore, P.A., and Lei, H. (2017). Genome editing abrogates angiogenesis *in vivo*. Nat. Commun. *8*, 112.

42. Amin, S.A., Adhikari, N., Gayen, S., and Jha, T. (2017). Homoisoflavonoids as potential antiangiogenic agents for retinal neovascularization. Biomed. Pharmacother. *95*, 818–827.

43. Liu, X., Li, Y., Liu, Y., Luo, Y., Wang, D., Annex, B.H., and Goldschmidt-Clermont, P.J. (2010). Endothelial progenitor cells (EPCs) mobilized and activated by neurotrophic factors may contribute to pathologic neovascularization in diabetic retinopathy. Am. J. Pathol. *176*, 504–515.

44. Shibuya, M. (2014). VEGF-VEGFR Signals in Health and Disease. Biomol. Ther. *22*, 1–9.

45. Muzyczka, N. (2010). Adeno-Associated Viral (AAV) Vectors: A Guide to Human Gene Therapy.

46. O'Reilly, M., Shipp, A., Rosenthal, E., Jambou, R., Shih, T., Montgomery, M., Gargiulo, L., Patterson, A., and Corrigan-Curay, J. (2012). NIH oversight of human gene transfer research involving retroviral, lentiviral, and adeno-associated virus vectors and the role of the NIH recombinant DNA advisory committee. Methods Enzymol. *507*, 313–335.

47. Bastola, P., Song, L., Gilger, B.C., and Hirsch, M.L. (2020). Adeno-Associated Virus Mediated Gene Therapy for Corneal Diseases. Pharmaceutics *12*, 767.

48. Handa, A., Muramatsu, S.I., Qiu, J., Mizukami, H., and Brown, K.E. (2000). Adeno-associated virus (AAV)-3-based vectors transduce haematopoietic cells not susceptible to transduction with AAV-2-based vectors. J. Gen. Virol. *81*, 2077–2084.

49. Colosi, P. (2006). High-efficiency Wild-type-free AAV Helper Functions.

50. (2013). Comparative Analysis of Adeno-Associated Virus Capsid Stability and Dynamics. J. Virol.

51. Thrasher, A.J., De Alwis, M., Casimir, C.M., Kinnon, C., Page, K., Lebkowski, J., Segal, A.W., and Levinsky, R.J. (1995). Generation of recombinant adeno-associated virus (rAAV) from an adenoviral vector and functional reconstitution of the NADPH-oxidase. Gene Ther. *2*, 481–485.

52. Duan, Y., Ma, G., Huang, X., D'Amore, P.A., Zhang, F., and Lei, H. (2016). The clustered, regularly interspaced, short palindromic repeats-associated endonuclease 9 (CRISPR/Cas9)-created MDM2 T309G mutation enhances vitreous-induced expression of MDM2 and proliferation and survival of cells. J. Biol. Chem. *291*, 16339–16347.

53. Tabebordbar, M., Zhu, K., Cheng, J.K.W., Chew, W.L., Widrick, J.J., Yan, W.X., Maesner, C., Wu, E.Y., Xiao, R., Ran, F.A., et al. (2016). In vivo gene editing in dystrophic mouse muscle and muscle stem cells. Science *351*, 407–411.

54. Han, H., Chen, N., Huang, X., Liu, B., Tian, J., and Lei, H. (2019). Phosphoinositide 3-kinase delta inactivation prevents vitreous-induced activation of AKT/MDM2/p53 and migration of retinal pigment epithelial cells. J. Biol. Chem. *294*, 15408–15417.

55. Qi, H., Dong, L., Fang, D., Chen, L., Wang, Y., Fan, N., Mao, X., Wu, W., Yan, X., Zhang, G., Zhang, S., and Lei, H. (2022). A Novel Role of IL13Rα2 in the Pathogenesis of Proliferative Vitreoretinopathy. Front. Med. *9*, 831436.

56. Liu, B., Song, J., Han, H., Hu, Z., and Lei, H. (2019). Blockade of MDM2 with Inactive Cas9 Prevents Epithelial to Mesenchymal Transition in Retinal Pigment Epithelial Cells. Lab. Invest.

57. Longchamp, A., Mirabella, T., Arduini, A., MacArthur, M.R., Das, A., Treviño-Villarreal, J.H., Hine, C., Ben-Sahra, I., Knudsen, N.H., Brace, L.E., et al. (2018). Amino Acid Restriction Triggers Angiogenesis via GCN2/ATF4 Regulation of VEGF and H(2)S Production. Cell *173*, 117–129.e14.

58. Majzoub, R.N., Chan, C.L., Ewert, K.K., Silva, B.F.B., Liang, K.S., and Safinya, C.R. (2015). Fluorescence microscopy colocalization of lipid-nucleic acid nanoparticles with wildtype and mutant Rab5-GFP: A platform for investigating early endosomal events. Biochim. Biophys. Acta *1848*, 1308–1318.